REVSTAT – Statistical Journal
Volume 0, Number 0, Month 0000, 000-000
https://doi.org/00.00000/revstat.v00i0.000

Extended Easily Changeable Kurtosis Distribution

Authors: Piotr Sulewski ✉
– Institute of Exact and Technical Sciences, Pomeranian University, Poland
piotr.sulewski@apsl.edu.pl

Received: Month 0000 Revised: Month 0000 Accepted: Month 0000

Abstract:

- This paper is the next step ahead in constructing probability distribution of changeable flatness of PDF that is expressed with well-known kurtosis measure. The distribution in question is named the Extended Easily Changeable Kurtosis and descends from the Easily Changeable Kurtosis. The paper covers PDF, CDF, modes and inflection points, quantiles, moments and Moors' measure and the Fisher Information Matrix. In addition generator of pseudo-random numbers that follow the Extended Easily Changeable Kurtosis is presented. Unknown parameters of the distribution are estimated with the maximum likelihood method. The paper ends with illustrative examples of applicability and flexibility of the new distribution. The most important R codes are presented in the supplementary material

Keywords:

- *normal distribution; modeling kurtosis; departure from normality.*

AMS Subject Classification:

- 60E05, 65C20.

✉ Corresponding author

1. INTRODUCTION

The statistics literature is filled with hundreds of continuous univariate distributions. However, in recent years, applications from the environmental, financial, biomedical sciences, engineering among others, have further shown that data sets following the classical distributions are more often the exception rather than the reality. Since there is a clear need for extended forms of these distributions a significant progress has been made toward the generalization of some well-known distributions and their successful application to problems in areas such as engineering, finance, economics and biomedical sciences, among others [1].

The article presents a symmetric distribution with two shape parameters $p > -1$ and $q > 0$ called the extended easily changeable kurtosis (EECK) distribution. As the name suggests, the $EECK(p > -1, q > 0)$ is an extended version of the easily changeable kurtosis (ECK) distribution with scale and shape parameters $a > 0$ and $p > -1$, respectively [31]. Instead of kurtosis γ_2, the article analyzes the excess kurtosis $\overline{\gamma}_2 = \gamma_2 - 3$, which can be positive or negative.

Symmetric distributions do not form such a big family as asymmetric distributions. Table 1 presents (in alphabetical order) thirty four symmetric distributions with the range of excess kurtosis $\overline{\gamma}_2$ and modality. Symmetric distributions with undefined excess kurtosis are: Cauchy [17], degenerate [12] and Voigt [32]. Symmetric distributions with constant excess kurtosis are: arcsine [19], bimodal normal [14], bimodal Laplace [14], cosine [24], hyperbolic secant [15], Laplace [15], logistic [3], normal [15], raised cosine [26], sine [9], semicircle [27], uniform [8], U-shaped [7]. Symmetric distributions with excess kurtosis in an finite interval: Bates [15], bimodal exponential power [14], bimodal power normal [5], ECK [31], extended normal [16], extended Laplace [15], extended t [15], Irwin-Hall [15], plasticizing component [30], Q-gaussian [34], t [15], Tukey with finite domain [10], U-power [7], Von Mises [21]. Symmetric distributions with excess kurtosis in an infinite interval are: generalized normal [23], normal-exponential-gamma [15], Tukey with infinite domain [10], U-quadratic [6]

The $ECK(a > 0, p > -1)$ [31], as the previous version of the $EECK(p > -1, q > 0)$, is unimodal distribution and can be used to model excess kurtosis in the range $(-2, 0)$.

The main goal of the paper is to define the distribution for excess kurtosis modeling in a larger range than $(-2, 0)$. As follows from the Malachov inequality $\overline{\gamma}_2 \geqslant \gamma_1^2 - 2$ [20], the best range would be the maximum range, i.e. $\langle -2, \infty)$.

The proposed distribution with $\overline{\gamma}_2^{EECK} \geq -2$ (see Subsection 2.4), like the generalized normal (GN) with $\overline{\gamma}_2^{GN} \geq -1.2$, normal-exponential-gamma (NEG) with $\overline{\gamma}_2^{NEG} > 0$ and Tukey (T) defined in an infinite domain with $\overline{\gamma}_2^{T} > 0$, belongs to the family of symmetrical, unimodal distributions with excess kurtosis values on infinite interval (see Table 1). In addition, the EECK is defined in the finite

Name	Modes	Range of $\bar{\gamma}_2$	Name	Modes	Range of $\bar{\gamma}_2$
Arcsine	2	-1.5	Logistic	1	6/5
Bates	1	$[-1.2,0)$	Normal	1	0
Bimodal exponential power	1,2	$[-3,3]$	Normal-exponential-gamma	1	$(0,\infty)$
Bimodal normal	2	$-4/3$	Plasticizing component	2	$(-2,0)$
Bimodal Laplace	2	1/3	Q-gaussian	1	$[-0.857,0]$
Bimodal power normal	1,2	$(-2,0)$ $\vee$ $(0,10.97)$	Raised cosine	1	$\frac{6(90-\pi^4)}{5(\pi^2-6)^2}$
Cauchy	1	-	Sine	1	$\frac{2(96-\pi^4)}{(\pi^2-8)^2}$
Cosine	1	0.251	Semicircle	1	-1
Degenerate	1	-	t	1	$(0,6]$
ECK	1	$(-2,0)$	Tukey[1]	1	$(0,\infty)$
Extended Normal	1,2	$[-4/3,0]$	Tukey[2]	1	$[-1.25,10.59]$
Extended Laplace	1,2	$(1/3,3]$	Uniform	∞	$-6/5$
Extended t	1,2	$[-4/3,6]$	U-power	2	$[-2,-1.81]$
Generalized normal	1	$[-1.2,0)$ $\vee$ $(0,\infty)$	U-quadratic	2	$(0,\infty)$
Hyperbolic secant	1	2	U-shaped	2	-1.5
Irwin–Hall	1	$[-1.2,0)$	Voigt	1	-
Laplace	1	3	Von Mises	1	$[-1.2,1.069]$

[1] infinite domain, [2] finite domain

Table 1: Symmetric distributions with range of excess kurtosis and modality

domain whereas the NEG, GN and T are defined in an infinite domain.

PDF of the NEG, as a mixture of normal distributions, has a complicated form and the analytical formula for excess kurtosis does not exist. PDF of the T distribution has a simple, closed form for a few exceptional values of the shape parameter, e.g. we get, respectively, for $\lambda = \{1, 0\}$ uniform and logistic distributions.

The analytical formulas for excess kurtosis of the EECK, GN and T distributions are respectively:

(1.1)

$$\bar{\gamma}_2^{EECK} = \frac{\Gamma^2\left(p+\frac{3}{q}\right)\Gamma\left(\frac{1}{q}\right)\Gamma\left(\frac{5}{q}\right)(pq+3)^2}{\Gamma^2\left(\frac{3}{q}\right)\Gamma\left(p+\frac{1}{q}\right)\Gamma\left(p+\frac{5}{q}\right)(pq+1)(pq+5)} - 3\,(p>-1, q>0)\,,$$

$$\overline{\gamma}_2^{GN} = \frac{\Gamma\left(\frac{5}{\beta}\right)\Gamma\left(\frac{1}{\beta}\right)}{\Gamma\left(\frac{3}{\beta}\right)^2} - 3\,(\beta > 0)\,, \tag{1.2}$$

$$\overline{\gamma}_2^{T} = \frac{(2\lambda+1)^2\,\Gamma(2\lambda+1)^2\left[3\Gamma(2\lambda+1)^2 + \Gamma(4\lambda+4) - 4\Gamma(3\lambda+1)\,\Gamma(\lambda+1)\right]}{(8\lambda+1)\,\Gamma(4\lambda+1)\left[\Gamma(\lambda+1)^2 - \Gamma(2\lambda+1)\right]^2} - 3\,(\lambda > -0.25) \tag{1.3}$$

The proof of (1.1) is presented in Subsection 2.4 (see Theorem 2.4).

Figure 1 shows the excess kurtosis of the EECK, GN and T distributions as a function of the shape parameters $p > -1$, $\beta > 0$ and $\lambda \in (-0.25, 0)$. The $\overline{\gamma}_2^{EECK}(p)$ is an increasing function similar to a linear function while $\overline{\gamma}_2^{GN}(\beta)$ and $\overline{\gamma}_2^{T}(\lambda)$ are initially decreasing strongly functions and then transforming into constant functions. This is especially visible for the GN distribution. The EECK and GN distributions can be used to model the negative and positive excess kurtosis. The negative values of excess kurtosis for the EECK and GN distributions are available on $[-2, 0]$ and $[-1.2, 0)$, respectively.

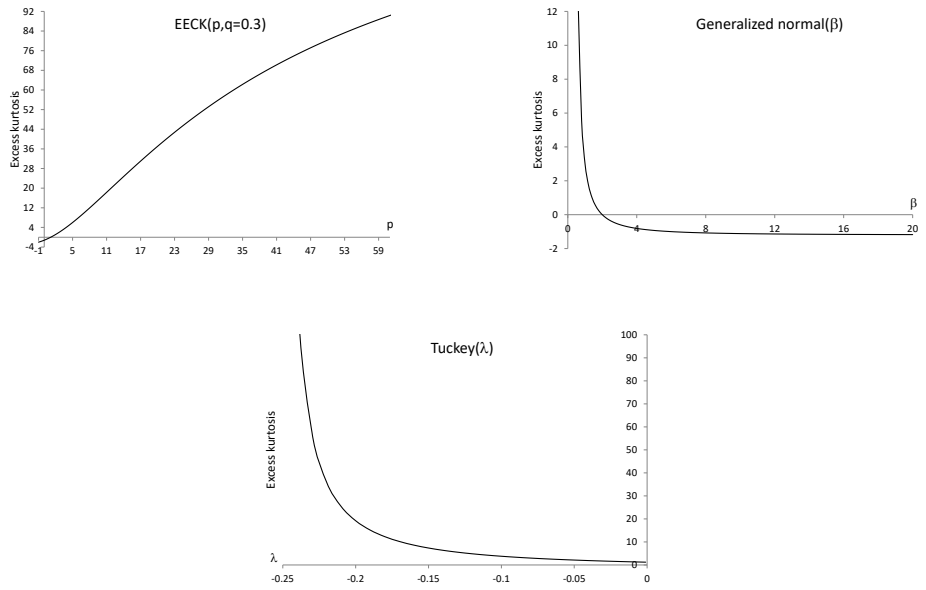

Figure 1: Excess kurtosis as a function of shape parameter

Formula (1.3) is the most complicated among formulas (1.1)-(1.3), however, for the EECK, GN, and T distributions, the shape parameter cannot be represented as a function of $\overline{\gamma}_2$, as is for the ECK and Q-gaussian distributions. This is the

price for expanding the range of $\overline{\gamma}_2$. Nowadays, in the era of advanced mathematical software, it is possible to compute the argument of a function knowing its value (using for example Mathcad or Microsoft Excel in newer versions).

Summarizing, the new proposal can be extremely useful when you want to seamlessly test the goodness-of-fit tests (GoFTs) ability to detect deviations from normality caused by the maximum range of excess kurtosis values, i.e. negative and positive. Real data example (see Section 4.2) demonstrates that the $EECK(p > -1, q > 0)$ distribution in the mixed variant is flexible and competitive model that deserves to be added to the existing distributions in data modeling.

Special cases of the $EECK(p > -1, q > 0)$ distribution are: the uniform, triangle and obviously $ECK(a > 0, p > -1)$. The $EECK(p > -1, q > 0)$ tends to the normal distribution (see Subsection 2.1).

It should also be mentioned that there is a group of asymmetric distributions, which are symmetrical for certain parameter values, e.q. the truncated normal, Birnbaum-Saunders [4], skew-normal [2], beta, two-piece normal [11], two-piece power normal [28] and plasticizing component [30].

This article is organized as follows. Section 2 presents the main properties of the EECK distribution such as PDF, CDF, modes, inflection points, quantiles, moments, Moors' measure, instructions to generate EECK pseudo-random numbers and the Fisher Information Matrix. The estimation procedures are provided in Section 3. The articles ends with applications and conclusions. The most important R codes are given in the supplementary material.

2. Main properties of introduced distribution

2.1. Distribution and density functions

Definition 1 The Eta function for $p > -1$ and $q > 0$ is defined as

$$H(p,q) = \int_{-1}^{1} [1 - |x|^q]^p \, dx = \frac{2B\left(\frac{1}{q}, p+1\right)}{q} = \frac{2\Gamma(p+1)\,\Gamma\left(\frac{1}{q}+1\right)}{\Gamma\left(p+\frac{1}{q}+1\right)}, \tag{2.1}$$

where $B(u,v)$ is the beta function.

Calculations in (2.1) were performed by the formula [13]

$$\int_0^1 x^{a-1}\left(1-x^b\right)^{c-1} dx = \frac{B\left(\frac{a}{b}, c\right)}{b}. \tag{2.2}$$

Exemplary values of the Eta function (2.1):

$$H(1,1)=1, H(0,1)=2, H(-0.5,1)=4, H(1,0.5)=\frac{2}{3}, H(0.5,1)=\frac{4}{3}.$$

Definition 2 The distribution of the random variable X with PDF given by

$$f(x;p,q)=\frac{[1-|x|^q]^p}{H(p,q)}, x\in\begin{cases}(-1,1) & \text{if } -1<p<0\\ [-1,1] & \text{if } p\geq 0\end{cases} \tag{2.3}$$

is called the extended easily changeable kurtosis (EECK) distribution, where $p>-1$ and $q>0$ are the shape parameters. The $EECK(p>-1,q>0)$ is symmetric around zero, since, based on (1.3) , $f(x;p,q)=f(-x;p,q)$ (see Figure 2). The $EECK(p>-1,q=2)$ is the $ECK(a=1,p>-1)$ [31].

The R codes of the dEECK function for computing PDF are provided in the supplementary material.

The standard deviation of the new proposal, based on (2.17), equals

$$\mu_2=\frac{(1+pq)\,\Gamma\left(\frac{3}{q}\right)\Gamma\left(p+\frac{1}{q}\right)}{(3+pq)\,\Gamma\left(\frac{1}{q}\right)\Gamma\left(p+\frac{3}{q}\right)}$$

therefore the $EECK(p,q)$ distribution tends to the normal distribution $N\left(0,\sqrt{\mu_2}\right)$ with PDF $\phi\left(x;0,\sqrt{\mu_2}\right)$

Let M (2.4) be the similarity measure of these distributions [29]. We have for $p>-1, q>0$

$$M(p,q)=\int_{-1}^{1}\min\left\{f(x;p,q),\phi\left[x;0,\sqrt{\frac{(1+pq)\,\Gamma\left(\frac{3}{q}\right)\Gamma\left(p+\frac{1}{q}\right)}{(3+pq)\,\Gamma\left(\frac{1}{q}\right)\Gamma\left(p+\frac{3}{q}\right)}}\right]\right\}dx. \tag{2.4}$$

The similarity measure M takes values on (0,1) and if PDFs are identical then $M=1$. For example $M(33,1)=0.871$, $M(33,1.5)=0.954$, $M(33,2)=0.995$, $M(33,2.5)=0.961$. A more detailed analysis of the value of the M measure showed that it has the highest values for $q=1.96$. We have $M(50,1.96)=0.999$.

The $EECK(p>-1,q>0)$ is the symmetrical distribution (Figure 2). The $EECK(p=0,q>0)$ is the uniform distribution $U(-1,1)$ (Figure 3, serie $p=0,q=1$. The $EECK(p>0,q>0)$ is unimodal with mode equals 0 (Figure 2, series $p=0.5,q=2$; $p=5,q=3$). The $EECK(-1<p<0,q>0)$ is pseudo $(-1<x<1)$ bimodal with bathtub shape (Figure 2, serie $p=-0.5,q=0.5$). The $EECK(p=1,q=1)$ is the triangle distribution (Figure 2, serie $p=1,q=1$). The $EECK(50,1.96)$ is in 99.9% the normal distribution $N(0,0.096)$ (Figure 2, serie $N(0,0.096)$).

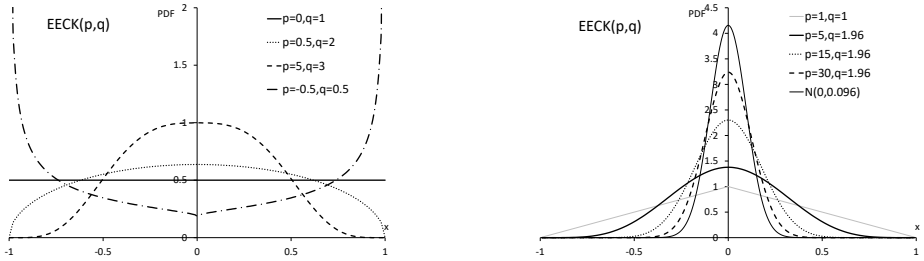

Figure 2: PDF of the $EECK(p,q)$ distribution for various parameter values

Theorem 2.1. If $X \sim EECK(p > -1, q > 0)$ with PDF $f(x;p,q)$ (2.3) then CDF of X is given by

$$F(x;p,q) = 0.5 + x\frac{{}_2F_1\left(-p, \frac{1}{q}, 1+\frac{1}{q}, |x|^q\right)}{H(p,q)} \tag{2.5}$$

where ${}_2F_1(a,b,c,x)$ is the Gaussian hypergeometric function.

Proof From (2.3) we have

$$\begin{aligned} F(x;p,q) &= \frac{1}{H(p,q)}\int_{-1}^{x}(1-|x|^q)^p\,dx \\ &= \frac{1}{H(p,q)}\left[\int_{-1}^{0}(1-|x|^q)^p\,dx + \int_{0}^{x}(1-|x|^q)^p\,dx\right]. \end{aligned} \tag{2.6}$$

To complete the proof, we need to calculate two integrals. The first one, based on (2.1), has the form

$$\int_{-1}^{0}(1-|x|^q)^p\,dx = 0.5H(p,q). \tag{2.7}$$

The second one can be written using a power series [13]

$$\int_{0}^{x}(1-|x|^q)^p\,dx = x\sum_{k=0}^{\infty}\frac{(-p)_k\left(\frac{1}{q}\right)_k}{\left(1+\frac{1}{q}\right)_k}\frac{|x|^{qk}}{k!} = {}_2F_1\left(-p,\frac{1}{q},1+\frac{1}{q},|x|^q\right)x \tag{2.8}$$

where ${}_2F_1(a,b,c,x)$ is the Gaussian hypergeometric function and $(x)_n$ is the Pochhammer symbol

$$(x)_n = \frac{\Gamma(x+n)}{\Gamma(x)} = x(x+1)...(x+n-1).$$

Substituting (2.7) and (2.8) to (2.6) we obtain (2.5). The proof is complete.

The R codes of the pEECK function for computing CDF are provided in the supplementary material.

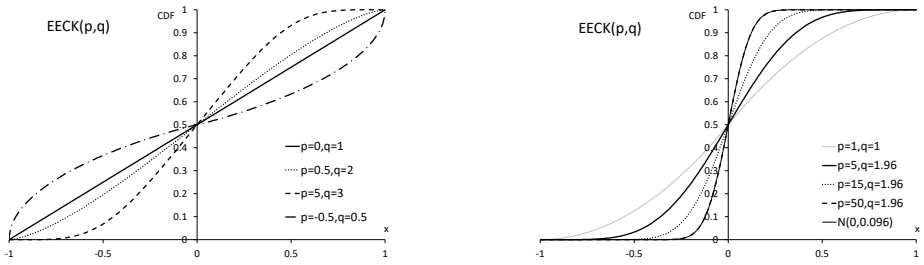

Figure 3: CDF of the $ECK(a,p)$ distribution for various parameter values

Figure 3 plots CDF of the $EECK(p>-1,q>0)$ distribution for some values of parameters. For $p=0$ we obtain the straight line (uniform distribution). For $p>0$ CDF is convex in $[-1,0)$ and is concave in $(0,1]$. For $-1<p<0$ CDF is concave in $(-1,0)$ and is convex in $(0,1)$. CDFs of the $EECK(50,1.96)$ distribution and $N(0,0.096)$ one coincide.

Theorem 2.2. The $EECK(p>-1,q>0)$ distribution with PDF given by (2.3) is identifiable in the parameter space $v=(p,q)$.

Proof Let $v_1=(p_1,q_1)$ and $v_2=(p_2,q_2)$. Let us suppose that $f_{v_1}(x)=f_{v_2}(x)$ for all x from support. This condition based on (2.1) and (2.3) implies that

$$\frac{q_1\left(1-|x|^{q_1}\right)^{p_1}}{2B\left(\frac{1}{q_1},p_1+1\right)}=\frac{q_2\left(1-|x|^{q_2}\right)^{p_2}}{2B\left(\frac{1}{q_2},p_2+1\right)} \tag{2.9}$$

If we apply log to both sides of (2.9) we obtain the system of three equations (2.10)

$$\log\left(\frac{q_1}{q_2}\right)=0, p_1\log\left(1-|x|^{q_1}\right)-p_2\log\left(1-|x|^{q_2}\right)=0, \log\left[\frac{B\left(\frac{1}{q_2},p_2+1\right)}{B\left(\frac{1}{q_1},p_1+1\right)}\right]=0.$$

From the first equation is $q_1=q_2$ and then from the second one is $p_1=p_2$. The proof is complete.

2.2. Modes and inflection points

Theorem 2.3. Let $X\sim EECK(p>-1,q>0)$. If $p=0$ then modal values $x_m\in[-1,1]$ (case of uniform distribution). If $p>0$ then $x_m=0$. If $-1<p<0$ then the $EECK(p,q)$ distribution is pseudo bimodal with modes $x_m(-1),x_m(1)$. The $f(x;p>0,q)$ (2.3) is monotonically increasing on the interval $(-1,0)$ and monotonically decreasing on the interval $(0,1)$. The $f(x;-1<p<0,q)$ (2.3) is

monotonically decreasing on the interval $(-1,0)$ and monotonically increasing on the interval $(0,1)$.

Proof Let $p \geq 0$ then PDF of the $EECK(p,q)$ distribution, based on (2.1) and (2.3), for any $x \in [-1,1]$ is given by

$$f(x;p,q) = \frac{\Gamma\left(p+\frac{1}{q}+1\right)}{2\Gamma(p+1)\,\Gamma\left(\frac{1}{q}+1\right)}\left(1-|x|^q\right)^p. \tag{2.11}$$

Let $p=0$ then $f(x;0,q) = \frac{\Gamma\left(\frac{1}{q}+1\right)}{2\Gamma\left(\frac{1}{q}+1\right)} = 0.5$ is constant in $[-1,1]$.

Let $p>0$ then

$$\frac{d}{dx}f(x;p,q) = \frac{\Gamma\left(p+\frac{1}{q}+1\right)}{2\Gamma(p+1)\,\Gamma\left(\frac{1}{q}+1\right)}p\left(1-|x|^q\right)^{p-1}\left[-q\,|x|^{q-1}\right]. \tag{2.12}$$

As a result of simple transformations $x_m = 0$ and (15) is positive on the interval $(-1,0)$ and negative on the interval $(0,1)$.

Let $-1 < p < 0$ then PDF (2.11) is defined for any $x \in (-1,1)$. As a result of simple transformations, (2.12) is negative on the interval $(-1,0)$ and positive on the the interval $(0,1)$. For x values very close to $-a$ and a PDF (2.8) has locally maximum values. The author of this article denotes these values as $x_m(-1), x_m(1)$ and proposed distribution defines as pseudo bimodal with modes at these points. The proof is complete.

Theorem 2.4. Let $X \sim ECK(p > -1, q > 0)$. The inflection points of the $f(x;p,q)$ (6) for $p>1 \wedge q>1$ or $-1<p<1 \wedge 0<q<1$ are given by means of the following formulas

$$x_1 = -\left(\frac{1-q}{1-pq}\right)^{\frac{1}{q}}, x_2 = \left(\frac{1-q}{1-pq}\right)^{\frac{1}{q}}. \tag{2.13}$$

Proof We can write (2.12) as

$$\frac{d}{dx}f(x;p,q) = \frac{-pq\Gamma\left(p+\frac{1}{q}+1\right)}{2\Gamma(p+1)\,\Gamma\left(\frac{1}{q}+1\right)}|x|^{q-1}\left(1-|x|^q\right)^{p-1}. \tag{2.14}$$

Let $A = \frac{-pq\Gamma\left(p+\frac{1}{q}+1\right)}{2\Gamma(p+1)\Gamma\left(\frac{1}{q}+1\right)}$ then (17) has the simpler form

$$\frac{d}{dx}f(x;p,q) = A\,|x|^{q-1}\left(1-|x|^q\right)^{p-1}.$$

The second derivative is given by

$$\frac{d^2}{dx^2} f(x;p,q) = A\left\{(q-1)|x|^{q-2}(1-|x|^q)^{p-1} - q|x|^{q-1}(p-1)(1-|x|^q)^{p-2}|x|^{q-1}\right\},$$

$$\frac{d^2}{dx^2} f(x;p,q) = A|x|^{q-2}(1-|x|^q)^{p-2}\left\{(q-1)(1-|x|^q) - q|x|(p-1)|x|^{q-1}\right\}.$$

thus

$$\frac{d^2}{dx^2} f(x;p,q) = 0 \Leftrightarrow (q-1)(1-|x|^q) - q|x|(p-1)|x|^{q-1} = 0.$$

As a result of simple transformations we have

$$x_1 = -\left(\frac{1-q}{1-pq}\right)^{\frac{1}{q}} \wedge x_1 > -1, x_2 = \left(\frac{1-q}{1-pq}\right)^{\frac{1}{q}} \wedge x_2 < 1, \tag{2.15}$$

then from (2.15) we obtain $p > 1 \wedge q > 1$ or $-1 < p < 1 \wedge 0 < q < 1$. The proof is complete.

2.3. Quantiles

Theorem 2.5. Let $X \sim EECK(p > -1, q > 0)$. The u-th $(0 < u < 1)$ quantile x_u is the solution of the following equation

$$(0.5-u)H(p,q) + {}_2F_1\left(-p, \frac{1}{q}, 1+\frac{1}{q}, |x_u|^q\right)x_u = 0, \tag{2.16}$$

where ${}_2F_1(a,b,c,x)$ is the Gaussian hypergeometric function and $H(p,q)$ is given by (2.1). The proposed distribution is symmetrical then $x_u = -x_{1-u}$, obviously and $x_{0.5} = 0$.

Proof Obtaining (19), based on the quantile definition, is trivial. The proof is complete.

The quantile x_u can be computed by numerical methods. The R codes of the qEECK function for computing the quantile x_u are provided in the supplementary material.

2.4. Moments and Moors' measure

Theorem 2.6. The k-th $(k = 0, 1, 2, \dots)$ non-central moments of the $EECK(p > -1, q > 0)$ distribution are given by

$$\alpha_k = \frac{\left[1+(-1)^k\right]B\left(\frac{k+1}{q}, p+1\right)}{qH(p,q)} = \frac{\left[1+(-1)^k\right]B\left(\frac{k+1}{q}, p+1\right)}{2B\left(\frac{1}{q}, p+1\right)}. \tag{2.17}$$

Proof The k-th ($k = 0, 1, 2, \dots$) non-central moments, based on (2.1) and (2.3), are defined as

(2.18)
$$\alpha_k = \frac{q}{2B\left(\frac{1}{q}, p+1\right)}\left[\int_{-1}^{0} x^k \left(1-|x|^q\right)^p dx + \int_{0}^{1} x^k \left(1-|x|^q\right)^p dx\right] = \frac{q\left(I_1+I_2\right)}{2B\left(\frac{1}{q}, p+1\right)}.$$

To solve the integrals I_1 and I_2, we have to use the integral formula (2.2). Thus:

$$I_1 = (-1)^k \frac{B\left(\frac{k+1}{q}, p+1\right)}{q}, I_2 = \frac{B\left(\frac{k+1}{q}, p+1\right)}{q} \tag{2.19}$$

and substituting obtained results into (2.18) we get (2.17). The proof is complete.

Theorem 2.7. The non-central moments $\alpha_k (k = 1, 3, \dots)$, variance μ_2 and excess kurtosis $\overline{\gamma}_2$ of the $EECK(p > -1, q > 0)$ distribution are given by

$$\alpha_k = 0\,(k = 1, 3, \ldots), \mu_2 = \frac{(1+pq)\,\Gamma\left(\frac{3}{q}\right)\Gamma\left(p+\frac{1}{q}\right)}{(3+pq)\,\Gamma\left(\frac{1}{q}\right)\Gamma\left(p+\frac{3}{q}\right)}, \tag{2.20}$$

$$\bar{\gamma}_2 = \frac{(pq+3)^2\,\Gamma\left(\frac{1}{q}\right)\Gamma\left(\frac{5}{q}\right)\Gamma\left(p+\frac{3}{q}\right)^2}{(pq+1)\,(pq+5)\,\Gamma\left(p+\frac{1}{q}\right)\Gamma\left(p+\frac{5}{q}\right)\Gamma\left(\frac{3}{q}\right)^2} - 3. \tag{2.21}$$

Proof The proof $\alpha_k = 0\,(k = 1, 3, \ldots)$, based on (2.17), is trivial.

The first non-central moment equals zero, so the non-central moments $\alpha_k\,(k = 0, 1, \ldots)$ are equal to the central moments $\mu_k\,(k = 0, 1, \ldots)$.

From (2.17), using the properties of the gamma function $\Gamma(x+1) = x\Gamma(x)$, we have

(2.22)
$$\alpha_2 = \mu_2 = \frac{B\left(\frac{3}{q}, p+1\right)}{B\left(\frac{1}{q}, p+1\right)} = \frac{\Gamma\left(\frac{3}{q}\right)\Gamma\left(p+\frac{1}{q}+1\right)}{\Gamma\left(\frac{1}{q}\right)\Gamma\left(p+\frac{3}{q}+1\right)} = \frac{(1+pq)\,\Gamma\left(\frac{3}{q}\right)\Gamma\left(p+\frac{1}{q}\right)}{(3+pq)\,\Gamma\left(\frac{1}{q}\right)\Gamma\left(p+\frac{3}{q}\right)},$$

(2.23)
$$\alpha_4 = \mu_4 = \frac{B\left(\frac{5}{q}, p+1\right)}{B\left(\frac{1}{q}, p+1\right)} = \frac{\Gamma\left(\frac{5}{q}\right)\Gamma\left(p+\frac{1}{q}+1\right)}{\Gamma\left(\frac{1}{q}\right)\Gamma\left(p+\frac{5}{q}+1\right)} = \frac{(1+pq)\,\Gamma\left(\frac{5}{q}\right)\Gamma\left(p+\frac{1}{q}\right)}{(5+pq)\,\Gamma\left(\frac{1}{q}\right)\Gamma\left(p+\frac{5}{q}\right)}.$$

Thus the excess kurtosis is given by

$$\bar{\gamma}_2 = \frac{\mu_4}{\mu_2^2} - 3 = \frac{(1+pq)\,\Gamma\left(\frac{5}{q}\right)\Gamma\left(p+\frac{1}{q}\right)}{(5+pq)\,\Gamma\left(\frac{1}{q}\right)\Gamma\left(p+\frac{5}{q}\right)} \frac{(3+pq)^2\,\Gamma\left(\frac{1}{q}\right)^2\Gamma\left(p+\frac{3}{q}\right)^2}{(1+pq)^2\,\Gamma\left(\frac{3}{q}\right)^2\Gamma\left(p+\frac{1}{q}\right)^2} - 3. \tag{2.24}$$

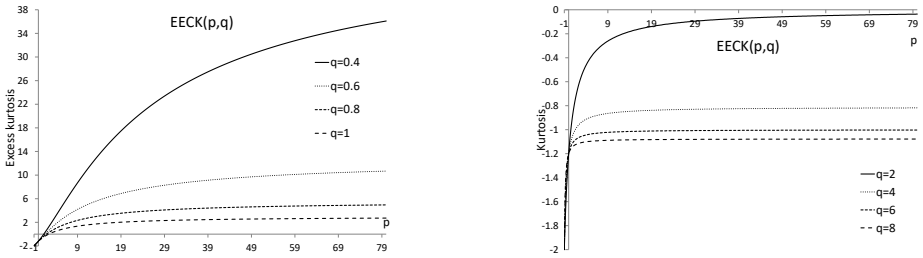

Figure 4: Excess kurtosis $\bar{\gamma}_2$ as a function of the shape parameter p

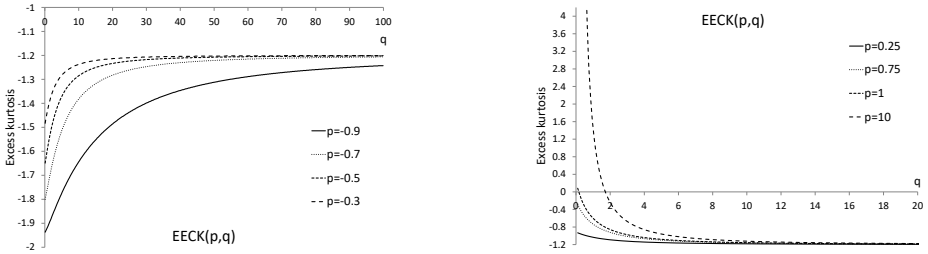

Figure 5: Excess kurtosis $\bar{\gamma}_2$ as a function of the shape parameter q

and we obtain (2.21) as a result of simple transformation. The proof is complete.

Figure 4 shows the excess kurtosis $\bar{\gamma}_2$ as a function of the shape parameter p for $q = 0.4, 0.6, 0.8, 1$ (left) and for $q = 2, 4, 6, 8$ (right). The excess kurtosis, according to the definition, varies in the range $[-2, \infty)$. The smaller q value, the higher excess kurtosis and the parameter p has a greater effect on the excess kurtosis.

Figure 5 shows the excess kurtosis $\bar{\gamma}_2$ as a function of the shape parameter q for $p = 0.3, 0.5, 0.7, 0.9$ (left) and for $p = 0.25, 0.75, 1, 10$ (right). For $p \in (-1, 0)$ the excess kurtosis tends from -2 to -1.2 when $q \to \infty$. For $p > 0$ kurtosis tends from ∞ to -1.2 when $q \to \infty$.

Moors [18] proposed a measure based on quantiles in the form

$$T = \frac{x_{7/8} - x_{5/8} + x_{3/8} - x_{1/8}}{x_{6/8} - x_{2/8}}, \tag{2.25}$$

where x_u is the solution of (2.16). The measure T is a quantile alternative for kurtosis and exists even for distribution for which no moments exist. Figure 6 shows the measure T as a function of the shape parameter p for $q = 0.75, 1, 2, 4$ (left) and as a function of the shape parameter q for $p = 0.75, 1, 2, 4$ (right). The $T(p)$ function decreases for $p\,(-1, 0)$ and increases for $p > 0$ mainly for its initial values. The $T(q)$ function tends to one.

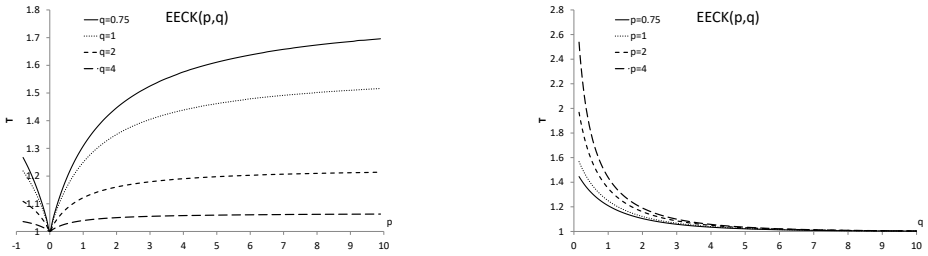

Figure 6: Moors' measure T as a function of the shape parameter p (left) and q (right)

2.5. Pseudo-random number generator

Let $X \sim EECK(p > -1, q > 0), R \sim U(0,1)$. The algorithm for generating n values of X, using the inverse CDF method, is as follows:

1. Repeat steps 1.1-1.4 n times:

    1.1 Let $R \sim U(0,1)$,

    1.2 Let $x = -1 + 0.01$,

    1.3 If $CDF(x; p, q) < R$, then $x = x + 0.01$,

    1.4 Return x,

where $CDF(x; p, q)$ is given by (2.5). It is obviously a universal algorithm for any distribution with $CDF(x; par)$, where par is the vector of distribution parameters.

The quantile function of the $EECK(p, q)$ does not have an analytical form, PDF (2.3) is non-negative on the interval $[-1, 1]$ and bounded by constant $d = f(0; p \geq 0, q)$, then we can use the von Neumann method, which in this case is much faster than the inverse CDF method. The algorithm for generating n values of X, using the von Neumann method [35], is as follows:

1. If $-1 < p < 0$ then use the inverse CDF method

2. If $p \geq 0$ then $d = f(0; p, q)$

3. Repeat steps 3.1-3.3 n times:

    3.1 Let $R_1 \sim U(-1, 1), R_2 \sim U(0, d)$,

    3.2 If $f(R_1; p, q) < R_2$ then goto Step 3.1 else $x = R_1$

3.3 Return x,

The R codes of the $rEECK$ and $rEECK1$ functions for generating n values of X are presented in the supplementary material.

2.6. Fisher Information Matrix

Theorem 2.8. The Fisher information matrix $I_{i,j}(i,j=1,2)$ for the $EECK(p>-1,q>0)$ distribution is given by

$$I_{11}=\left[A-B+\widetilde{H}\left(p\right)-\widetilde{H}\left(p+\frac{1}{q}\right)\right]^{2}+\Psi_{1}\left(p+1\right)-\Psi_{1}\left(p+\frac{1}{q}+1\right), \tag{2.26}$$

$$I_{12}=I_{21}=\frac{\left(A-B\right)\left(C-A\right)}{q^{2}}-\frac{\left(A-B\right)\Gamma\left(p+\frac{1}{q}+1\right)}{\Gamma\left(p+1\right)\Gamma\left(\frac{1}{q}+1\right)} +\frac{\left(C-A\right)\left[\widetilde{H}\left(p\right)-\widetilde{H}\left(p+\frac{1}{q}\right)\right]}{q^{2}}+\frac{\Gamma\left(p+\frac{1}{q}+1\right)}{p\Gamma\left(p+1\right)\Gamma\left(\frac{1}{q}+1\right)}, \tag{2.27}$$

$$I_{22}=\frac{\left(C-A\right)^{2}}{q^{4}}-\frac{2\left(C-A\right)\Gamma\left(p+\frac{1}{q}+1\right)}{q^{3}\Gamma\left(p+1\right)\Gamma\left(\frac{1}{q}+1\right)}+\frac{pq^{2}\left(pq+1\right)\Gamma\left(2-\frac{1}{q}\right)\Gamma\left(p+\frac{1}{q}\right)}{\left(p-1\right)\left(pq-1\right)\Gamma\left(p-\frac{1}{q}\right)\Gamma\left(\frac{1}{q}\right)}, \tag{2.28}$$

where $\widetilde{H}\left(z\right)=\sum_{k=1}^{z}\frac{1}{k}$ is the harmonic function, $\Psi_{n}\left(z\right)$ is the n^{th} derivative of the digamma function $\Psi\left(z\right)$, $A=\Psi\left(p+\frac{1}{q}+1\right),B=\Psi\left(p+1\right),C=\Psi\left(\frac{1}{q}+1\right)$ as well as $I_{11},I_{12}=I_{21},I_{22}$ are defined for $(p>-1,q>0)$, $(p>0,q>0)$ and $(p>1,q>0.5)$ respectively.

Proof First, we need to take the logarithm. From (5) we have

$$\ln\left[f\left(x;p,q\right)\right]=\ln\left[\Gamma\left(p+\frac{1}{q}+1\right)\right]+p\ln\left(1-\left|x\right|^{q}\right)-\ln\left[2\Gamma\left(p+1\right)\right]-\ln\Gamma\left(\frac{1}{q}+1\right)$$

Second, we need to calculate the partial derivatives

$$\frac{d\ln\left[f\left(x;p,q\right)\right]}{dp}=\Psi\left(p+\frac{1}{q}+1\right)+\ln\left(1-\left|x\right|^{q}\right)-\Psi\left(p+1\right),$$

$$\frac{d\ln\left[f\left(x;p,q\right)\right]}{dq}=\frac{-1}{q^{2}}\Psi\left(p+\frac{1}{q}+1\right)-\frac{pq\left|x\right|^{q-1}}{1-\left|x\right|^{q}}+\frac{1}{q^{2}}\Psi\left(\frac{1}{q}+1\right).$$

Hence, we get the Fisher score in the form

$$\boldsymbol{h}\left(\boldsymbol{x};\boldsymbol{p},\boldsymbol{q}\right)=\begin{bmatrix}A-B+\ln\left(1-\left|x\right|^{q}\right)\\ \frac{C-A}{q^{2}}-\frac{pq\left|x\right|^{q-1}}{1-\left|x\right|^{q}}\end{bmatrix}$$

Let $\boldsymbol{u}(x;p,q)=\boldsymbol{h}(x;p,q)\,\boldsymbol{h}(x;p,q)^{T}$ then

$$u_{11}=\left[A-B+\ln\left(1-|x|^{q}\right)\right]^{2},u_{22}=\left[\frac{C-A}{q^{2}}-\frac{pq\,|x|^{q-1}}{1-|x|^{q}}\right]^{2},$$

$$u_{12}=u_{21}=\left[A-B+\ln\left(1-|x|^{q}\right)\right]\left[\frac{C-A}{q^{2}}-\frac{pq\,|x|^{q-1}}{1-|x|^{q}}\right].$$

Let $I_{i,j}=E\left[u_{i,j}\right](i,j=1,2)$ then

$$I_{11}=(A-B)^{2}+2(A-B)\,E\left[\ln\left(1-|x|^{q}\right)\right]+E\left[\ln^{2}\left(1-|x|^{q}\right)\right], \tag{2.29}$$

(2.30)

$$I_{12}=I_{21}=\frac{(A-B)(C-A)}{q^{2}}-pq(A-B)\,E\left[\frac{|x|^{q-1}}{1-|x|^{q}}\right]+\frac{C-A}{q^{2}}E\left[\ln\left(1-|x|^{q}\right)\right]$$
$$-pqE\left[\frac{|x|^{q-1}\ln\left(1-|x|^{q}\right)}{1-|x|^{q}}\right],$$

$$I_{22}=\frac{(C-A)^{2}}{q^{4}}-\frac{2p(C-A)}{q^{2}}E\left[\frac{|x|^{q-1}}{1-|x|^{q}}\right]+p^{2}q^{2}E\left[\frac{|x|^{2q-2}}{\left(1-|x|^{q}\right)^{2}}\right]. \tag{2.31}$$

To write the Fisher Information Matrix in a simpler form, we use (2.2) and Mathematica software. We obtain:

(2.32)

$$E\left[\ln\left(1-|x|^{q}\right)\right]=\frac{\Gamma\left(p+\frac{1}{q}+1\right)}{2\Gamma(p+1)\,\Gamma\left(\frac{1}{q}+1\right)}\int_{-1}^{1}\frac{\ln\left(1-|x|^{q}\right)}{\left(1-|x|^{q}\right)^{-p}}dx=\widetilde{H}(p)-\widetilde{H}\left(p+\frac{1}{q}\right),$$

(2.33)

$$E\left[\ln^{2}\left(1-|x|^{q}\right)\right]=\frac{\Gamma\left(p+\frac{1}{q}+1\right)}{2\Gamma(p+1)\,\Gamma\left(\frac{1}{q}+1\right)}\int_{-1}^{1}\frac{\ln^{2}\left(1-|x|^{q}\right)}{\left(1-|x|^{q}\right)^{-p}}dx=\frac{\Gamma\left(p+\frac{1}{q}+1\right)}{2\Gamma(p+1)\,\Gamma\left(\frac{1}{q}+1\right)}$$
$$\cdot\frac{2\Gamma(p+1)\,\Gamma\left(\frac{1}{q}+1\right)}{\Gamma\left(p+\frac{1}{q}+1\right)}\left\{\left[\widetilde{H}(p)-\widetilde{H}\left(p+\frac{1}{q}\right)\right]^{2}+\Psi_{1}(p+1)-\Psi_{1}\left(p+\frac{1}{q}+1\right)\right\}$$
$$=\left[\widetilde{H}(p)-\widetilde{H}\left(p+\frac{1}{q}\right)\right]^{2}+\Psi_{1}(p+1)-\Psi_{1}\left(p+\frac{1}{q}+1\right),$$

(2.34)

$$E\left[\frac{|x|^{q-1}}{1-|x|^{q}}\right]=\frac{\Gamma\left(p+\frac{1}{q}+1\right)}{2\Gamma(p+1)\,\Gamma\left(\frac{1}{q}+1\right)}\int_{-1}^{1}\frac{|x|^{q-1}}{\left(1-|x|^{q}\right)^{-p+1}}dx=\frac{\Gamma\left(p+\frac{1}{q}+1\right)}{pq\Gamma(p+1)\,\Gamma\left(\frac{1}{q}+1\right)},$$

(2.35)
$$E\left[\frac{|x|^{q-1}\ln\left(1-|x|^{q}\right)}{1-|x|^{q}}\right]=\frac{\Gamma\left(p+\frac{1}{q}+1\right)}{2\Gamma\left(p+1\right)\Gamma\left(\frac{1}{q}+1\right)}\int_{-1}^{1}\frac{|x|^{q-1}\ln\left(1-|x|^{q}\right)}{\left(1-|x|^{q}\right)^{-p+1}}dx=$$
$$=\frac{\Gamma\left(p+\frac{1}{q}+1\right)}{2\Gamma\left(p+1\right)\Gamma\left(\frac{1}{q}+1\right)}\frac{-2}{p^{2}q}=\frac{-\Gamma\left(p+\frac{1}{q}+1\right)}{p^{2}q\Gamma\left(p+1\right)\Gamma\left(\frac{1}{q}+1\right)}$$

(2.36)
$$E\left[\frac{|x|^{2q-2}}{\left(1-|x|^{q}\right)^{2}}\right]=\frac{\Gamma\left(p+\frac{1}{q}+1\right)}{2\Gamma\left(p+1\right)\Gamma\left(\frac{1}{q}+1\right)}\int_{-1}^{1}\frac{|x|^{2q-2}}{\left(1-|x|^{q}\right)^{-p+2}}dx=$$
$$=\frac{\Gamma\left(p+\frac{1}{q}+1\right)}{2\Gamma\left(p+1\right)\Gamma\left(\frac{1}{q}+1\right)}\frac{2\Gamma\left(p-1\right)\Gamma\left(2-\frac{1}{q}\right)}{q\Gamma\left(1+p-\frac{1}{q}\right)}=\frac{\left(pq+1\right)\Gamma\left(2-\frac{1}{q}\right)\Gamma\left(p+\frac{1}{q}\right)}{p\left(p-1\right)\left(pq-1\right)\Gamma\left(p-\frac{1}{q}\right)\Gamma\left(\frac{1}{q}\right)}.$$

Substituting formulas (2.32)-(2.36) into formulas (2.29)-(2.31), as a result of simple transformations, we get formulas (2.26)-(2.28). The proof is complete.

3. Maximum likelihood estimation

Let $x_1^*, x_2^*, ..., x_n^*$ be a random sample size n from the $EECK(p>-1, q>0)$ distribution. Our target is to estimate the unknown values of the parameters p, q. The likelihood function based on (2.3) is given by

$$L=\prod_{i=1}^{n}f\left(x_i^*;p,q\right)=\frac{\Gamma\left(p+\frac{1}{q}+1\right)}{2\Gamma\left(p+1\right)\Gamma\left(\frac{1}{q}+1\right)}\prod_{i=1}^{n}\left(1-|x_i^*|^{q}\right)^{p},$$

then the log-likelihood function is defined as

(3.1)
$$l=n\ln\left[\Gamma\left(p+\frac{1}{q}+1\right)\right]-n\ln\left[2\Gamma\left(p+1\right)\right]-n\ln\left[\Gamma\left(\frac{1}{q}+1\right)\right]+p\sum_{i=1}^{n}\ln\left(1-|x_i^*|^{q}\right)$$

and

(3.2)
$$\frac{dl}{dp}=n\Psi\left(p+\frac{1}{q}+1\right)-n\Psi\left(p+1\right)+\sum_{i=1}^{n}\ln\left(1-|x_i^*|^{q}\right)=0,$$

(3.3)
$$\frac{dl}{dq}=\frac{-n}{q^{2}}\Psi\left(p+\frac{1}{q}+1\right)+\frac{n}{q^{2}}\Psi\left(\frac{1}{q}+1\right)-\frac{npq\,|x_i^*|^{q-1}}{1-|x_i^*|^{q}}=0.$$

where Ψ is the digamma function.

The maximum likelihood estimates (MLEs) are solutions of the system equations (3.2)-(3.3). We have

$$\frac{1}{n}\sum_{i=1}^{n}\ln\left(1-|x_i^*|^q\right)=\Psi\left(p+1\right)-\Psi\left(p+\frac{1}{q}+1\right), \tag{3.4}$$

$$\Psi\left(\frac{1}{q}+1\right)-\Psi\left(p+\frac{1}{q}+1\right)=-\frac{pq^3\,|x_i^*|^{q-1}}{1-|x_i^*|^q}. \tag{3.5}$$

Solving the system equations (3.2)-(3.3) with numerical method we have obtain $\hat{p},\hat{q}$. We can also maximize the log-likelihood function (3.1) to obtain the MLEs of the p,q parameters.

The biases and the root mean squared errors (RMSEs) of the MLEs are shown in Tables 2 and 3. The simulation study was performed with 10^3 samples using sample sizes of $100, 150, 200$. The samples were drawn from the $EECK(p,3)$, where $p=1,2,3$ (see Table 2) and from the $EECK(3,q)$, where $q=1,2,3$ (see Table 3). We observe that the estimates approach true values when the sample size increases, it implies the consistency of the estimates. The biases of the $\hat{p}$ and $\hat{q}$ diminish for large samples and are smaller for $\hat{q}$ than for $\hat{p}$. The RMSEs decrease with the value of p for $\hat{q}$ (see Table 2).

		$\widehat{p}$		$\widehat{q}$	
p	**n**	**Bias**	**RMSE**	**Bias**	**RMSE**
1	100	0.555	2.820	0.443	3.593
	150	0.296	1.802	0.186	2.992
	200	0.110	1.172	-0.081	2.279
2	100	0.965	4.408	0.379	2.313
	150	0.724	2.739	0.339	1.908
	200	0.338	1.468	0.110	1.397
3	100	1.255	3.875	0.336	1.701
	150	0.892	3.126	0.269	1.441
	200	0.712	2.289	0.259	1.261

Table 2: Biases and RMSEs of the MLEs from the $EECK(p,3)$

To examine the accuracy of the coverage probability of the asymptotic confidence intervals (CIs), another simulation study was performed with 10^3 samples using sample sizes of $100, 150, 200$. The study focused on the parameters p,q and samples drawn from the $EECK(p=3,q=3)$. The coverage probabilities of the obtained 95% CIs for $p=3,q=3$ reported in Table 4 are very close to the nominal level. The results suggested that the obtained standard errors and hence the asymptotic CIs are reliable.

		$\widehat{p}$		$\widehat{q}$	
q	**n**	**Bias**	**RMSE**	**Bias**	**RMSE**
1	100	0.266	5.510	0.485	3.361
	150	0.011	1.202	0.231	2.169
	200	-0.125	0.320	-0.034	1.290
2	100	0.173	1.168	0.531	3.600
	150	0.046	0.873	0.176	3.234
	200	-0.020	0.711	-0.044	2.729
3	100	0.264	2.584	0.439	5.733
	150	0.149	1.586	0.209	5.283
	200	0.047	1.005	0.029	4.544

Table 3: Biases and RMSEs of the MLEs from the $EECK(0.5, q)$

n	**p**	**q**
100	0.954	0.942
150	0.938	0.945
200	0.957	0.96

Table 4: Coverage probability for the standard asymptotic 95% CIs, $EECK(p = 3, q = 3)$

4. Application

This section is divided into two subsections. We present examples of the applicability and flexibility of the $EECK(p > -1, q > 0)$. Subsection 4.1 is devoted to GoFTs, Subsection 4.2 deals with fitting distributions to data.

4.1. Comparison of goodness-of-fit tests

As it was mentioned in Introduction, the shape parameter of the EECK distribution cannot be represented as a function of $\overline{\gamma}_2$, as is for the ECK distribution [31]. Recall, however, that the ECK excess kurtosis takes values on interval $(-2, 0)$, while the EECK excess kurtosis has values on interval $[-2, \infty)$. Using e.g. Mathcad, you can easily calculate the argument of a function knowing its value.

The EECK distribution can be extremely useful when you want to seamlessly test GoFTs ability to detect deviations from normality caused by a negative and positive excess kurtosis.

Let $x_{(1)}, x_{(2)}, ..., x_{(n)}$ be an ordered random sample of size n. Seven GoFTs were selected to be subjects of the Monte Carlo simulation. Five of them as being

very popular GoFTs have been implemented in the R software. These tests are: Shapiro-Wilk (SW), Kolmogorov-Smirnov (KS), Cramer-von Mises (CVM), Anderson-Darling (AD) and Shapiro - Francia (SF). Two tests not implemented yet, probably for their novelty, are: H_n [33] and LF_m [29] tests.

The H_n test statistic is defined as

$$H_n = \frac{1}{n}\sum_{i=1}^{n} h\left[\frac{1+\Phi\left(\frac{x_{(i)}-\overline{x}}{s},0,1\right)}{1+\frac{i}{n}}\right], h\left(x\right) = \left(\frac{x-1}{x+1}\right)^2, \tag{4.1}$$

where $\overline{x}$ and s^2 are the sample mean and sample variance, respectively.

The LF_m test statistic is given by

$$LF_m = \max\left|\frac{i-\overline{\alpha}}{n-\overline{\alpha}-\overline{\beta}+1} - \Phi\left(\frac{x_{(i)}-\overline{x}}{s},0,1\right)\right|, \left(\overline{\alpha},\overline{\beta}\geq 1\right). \tag{4.2}$$

If an alternatively distribution is both symmetric and of negative (positive) excess kurtosis $\overline{\alpha}=\overline{\beta}=0$ ($\overline{\alpha}=\overline{\beta}=1$) are recommended.

The similarity measure M (2.4) of $N(0, 0.096)$ and $EECK(p = 50, 1.96)$, as was mentioned in Subsection 2.1, is 0.999. In the legend of Figure 7, the values of the similarity measure M of the normal distribution and the EECK are given. Figure 17 (left) shows PDF of the $N\left(0, 0.096\right)$ and $EECK(p, 1.96)$ distributions. For the presented values of the shape parameters, an excess kurtosis of the EECK is negative (see Table 5). If p increases, the similarity measure also increases. Figure 7 (right) shows PDF of the $N\left(0, 0.297\right)$ and $EECK(p, 1.3)$ distributions. The similarity measure M of $N(0, 0.297)$ and $EECK(p = 2.75, 1.3)$ is 0.999

For the presented values of the shape parameters, an excess kurtosis of the EECK is positive (see Table 6). If p decreases, the similarity measure M increases.

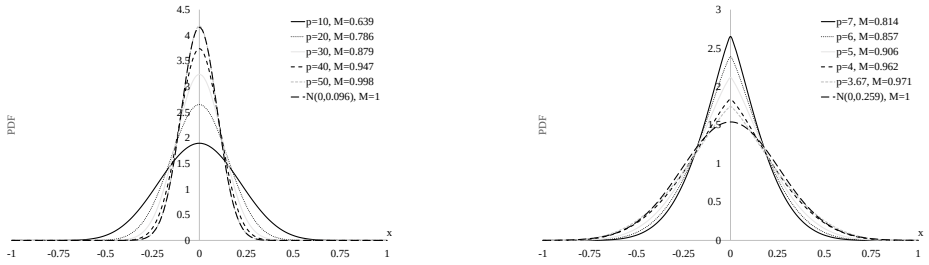

Figure 7: The $EECK(p, q)$ distribution with values of the similarity measure M to the normal distribution

Table 5 (Table 6) shows the modeling of negative (positive) excess kurtosis, i.e. for a given value of $\overline{\gamma}_2$ of the $EECK(p, 1.96)$ ($EECK(p, 1.3)$) the value of the shape parameter p is caclulated.

	EECK(p,1.96)									N(0,0.096)
$\overline{\gamma}_2$	-1	-0.75	-0.5	-0.4	-0.3	-0.2	-0.1	-0.05	-0.025	0
p	0.49	1.451	3.3	4.627	6.731	10.58	19.882	32.188	45.316	-

Source: Own material.

Table 5: Modeling of negative excess kurtosis $\overline{\gamma}_2$. $EECK(p, 1.96)$

	EECK(p,1.3)									N(0,0.259)
$\overline{\gamma}_2$	0.5	0.4	0.3	0.2	0.1	0.05	0.025	0.01	0.005	0.001	0
p	8.261	6.95	5.891	5.018	4.286	3.963	3.81	3.721	3.693	3.669	-

Source: Own material.

Table 6: Modeling of negative excess kurtosis $\overline{\gamma}_2$. $EECK(p, 1.3)$

Phase 1: In this phase the aim is to investigate to what degree selected GoFTs listed in Table 7 are able to distinct between the normal and proposed distributions. In other words the aim is to determine powers of GoFTs being under discussion when samples come from $EECK(p, q)$ general populations. For the aim to be accomplished, critical values $cv_{0.05}$ ascribed to GoFTs (where $\alpha = 0.05$ is the test significance level) were needed. These critical values were estimated with the Monte Carlo method. Seven large scale experiments were performed each of which devoted to one of GoFT. Each experiment consisted of generating 10^5 samples of sizes $n = 20, 40, 60$. The samples followed the $N(0, 0.096)$ and $N(0, 0.297)$ distributions. Each sample was tested for normality. Obtained in this way values of test statistics (denoted $Q_i\,(i = 1, 2, ..., m)$ were collected an then ranked. Critical values were assessed according to the formula $cv_{0.05} = Q_{[\alpha m]}$.

Table 7 present obtained $cv_{0.05}$ critical values. Tables 8 and 9, in turn, present relevant test powers when samples come from the $EECK(p, q)$ general populations. Each experiment consisted of generating 10^5 samples of sizes $n = 20, 40, 60$. The shape parameter is $q = 1.96 (q = 1.3)$. Values of the shape parameter p were listed in Table 5 (Table 6).

The conclusions from Tables 8 and 9 are very interesting. For $n = 20$, the LF, CvM, AD, SW, Hn tests detect only $\overline{\gamma}_2 = -1$, LFm - $\overline{\gamma}_2 = -0.75$; LFm, SF tests detect even $\overline{\gamma}_2 = 0.001$. For $n = 40$, the LF, CvM, AD, SW, Hn and

n	**20**		**40**		**60**	
s	**0.096**	**0.259**	**0.096**	**0.259**	**0.096**	**0.259**
LF	0.19177	0.19202	0.13841	0.13844	0.11385	0.11376
CVM	0.12278	0.12223	0.12445	0.12446	0.12490	0.12484
AD	0.72300	0.71959	0.73751	0.73840	0.74215	0.74084
SW	0.98287	0.98282	0.98860	0.98861	0.99140	0.99139
SF	0.98464	0.98469	0.99003	0.99007	0.99248	0.99249
Hn	0.00077	0.00076	0.00038	0.00038	0.00025	0.00025
LFm	0.16195	0.17471	0.12388	0.12895	0.10450	0.10726

Table 7: Critical values $cv_{0.05}$ for GoFTs. The samples of size n followed the $N(0, s)$

GoFT		$\bar{\gamma}_2$									
		−1	−0.75	−0.5	−0.4	−0.3	−0.2	−0.1	−0.05	−0.025	0
		p									
	n	0.49	1.451	3.3	4.627	6.731	10.58	19.882	32.188	45.316	-
LF	20	0.063	0.046	0.044	0.045	0.045	0.048	0.048	0.049	0.050	0.050
	40	0.099	0.058	0.048	0.045	0.047	0.047	0.049	0.049	0.050	0.050
	60	0.148	0.074	0.052	0.049	0.047	0.047	0.049	0.051	0.050	0.051
CVM	20	0.074	0.047	0.044	0.042	0.044	0.047	0.047	0.049	0.050	0.050
	40	0.144	0.069	0.049	0.045	0.045	0.046	0.048	0.049	0.049	0.050
	60	0.237	0.095	0.055	0.049	0.046	0.046	0.049	0.049	0.049	0.051
AD	20	0.079	0.047	0.041	0.040	0.042	0.045	0.047	0.048	0.050	0.050
	40	0.178	0.075	0.048	0.043	0.044	0.044	0.047	0.049	0.048	0.050
	60	0.311	0.109	0.057	0.048	0.045	0.045	0.048	0.049	0.048	0.050
SW	20	0.083	0.043	0.036	0.038	0.039	0.041	0.045	0.048	0.048	0.049
	40	0.223	0.071	0.040	0.036	0.036	0.038	0.043	0.046	0.049	0.051
	60	0.429	0.115	0.047	0.039	0.037	0.037	0.043	0.045	0.046	0.051
SF	20	0.034	0.022	0.025	0.030	0.033	0.039	0.045	0.049	0.050	0.049
	40	0.083	0.025	0.019	0.021	0.025	0.032	0.041	0.045	0.050	0.052
	60	0.195	0.040	0.019	0.020	0.023	0.028	0.040	0.045	0.047	0.051
H_n	20	0.075	0.049	0.043	0.044	0.044	0.046	0.047	0.048	0.049	0.049
	40	0.154	0.074	0.051	0.046	0.047	0.046	0.048	0.049	0.049	0.051
	60	0.259	0.105	0.059	0.053	0.049	0.050	0.051	0.051	0.050	0.053
LF_m	20	0.082	0.056	0.050	0.049	0.048	0.050	0.049	0.049	0.051	0.051
	40	0.125	0.073	0.054	0.050	0.051	0.049	0.051	0.050	0.050	0.051
	60	0.181	0.087	0.059	0.053	0.051	0.049	0.050	0.051	0.050	0.051

Table 8: Powers of tests at $\alpha = 0.05$, when the $EECK(p, 1.96)$ is the actual population distribution. The case of negative excess kurtosis values

LFm tests detect only $\overline{\gamma}_2 = -0.75$; LF, CvM, AD, Hn, and LFm tests detect even $\overline{\gamma}_2 = 0.001$. For n=60, the AD, Hn and LFm tests detect only $\overline{\gamma}_2 = -0.5$; LF and CVM tests detect only $\overline{\gamma}_2 = -0.75$; LF, CvM, AD, Hn, and LFm tests detect even $\overline{\gamma}_2 = 0.001$.

In Phase 1, we showed that the considered GoFTs detect positive excess kurtosis better than negative one.

Phase 2. In this phase the aim is to investigate to what degree an undetected excess kurtosis impacts the performance of two basic tests related to parameters

GoFT		$\bar{\gamma}_2$										
		0.5	0.4	0.3	0.2	0.1	0.05	0.025	0.01	0.005	0.001	0
		p										
	n	8.261	6.95	5.891	5.018	4.286	3.963	3.810	3.721	3.693	3.669	-
LF	20	0.072	0.069	0.064	0.060	0.055	0.056	0.053	0.054	0.054	0.053	0.050
	40	0.089	0.081	0.074	0.070	0.061	0.060	0.058	0.056	0.055	0.057	0.051
	60	0.105	0.094	0.084	0.075	0.065	0.062	0.060	0.060	0.060	0.060	0.052
CVM	20	0.081	0.077	0.071	0.063	0.059	0.057	0.056	0.056	0.054	0.055	0.052
	40	0.101	0.091	0.080	0.073	0.064	0.060	0.059	0.056	0.056	0.056	0.049
	60	0.122	0.108	0.093	0.082	0.068	0.063	0.062	0.061	0.060	0.061	0.051
AD	20	0.082	0.077	0.071	0.062	0.057	0.054	0.055	0.054	0.052	0.053	0.052
	40	0.101	0.090	0.079	0.071	0.062	0.058	0.056	0.054	0.053	0.053	0.049
	60	0.124	0.107	0.092	0.081	0.066	0.061	0.060	0.058	0.057	0.059	0.051
SW	20	0.081	0.073	0.067	0.060	0.052	0.051	0.049	0.048	0.047	0.050	0.050
	40	0.098	0.085	0.074	0.060	0.052	0.047	0.045	0.044	0.044	0.048	0.050
	60	0.114	0.095	0.079	0.064	0.050	0.045	0.044	0.042	0.042	0.046	0.051
SF	20	0.102	0.092	0.081	0.072	0.062	0.058	0.055	0.055	0.052	0.057	0.049
	40	0.127	0.111	0.093	0.074	0.061	0.053	0.049	0.048	0.049	0.053	0.049
	60	0.148	0.125	0.102	0.078	0.058	0.050	0.047	0.045	0.044	0.051	0.052
H_n	20	0.078	0.073	0.068	0.061	0.058	0.056	0.055	0.054	0.053	0.055	0.052
	40	0.094	0.084	0.076	0.069	0.061	0.058	0.056	0.055	0.054	0.054	0.049
	60	0.118	0.105	0.091	0.080	0.067	0.063	0.061	0.060	0.059	0.061	0.053
LF_m	20	0.082	0.078	0.073	0.066	0.061	0.060	0.057	0.057	0.057	0.057	0.050
	40	0.100	0.091	0.082	0.076	0.066	0.064	0.062	0.060	0.059	0.060	0.050
	60	0.116	0.104	0.092	0.081	0.069	0.066	0.064	0.064	0.063	0.063	0.051

Table 9: Powers of tests at $\alpha = 0.05$, when the $EECK(p, 1.3)$ is the actual population distribution. The case of positive excess kurtosis values

of the Normal distribution, namely Student t test and Fisher–Snedecor F test.

Let $x_{1,1}, x_{1,2}, ..., x_{1,n}$ and $x_{2,1}, x_{2,2}, ..., x_{2,n}$ be two samples of sizes n drawn from particular general populations. Let us remember that t and F test statistics have the following forms:

$$\dot{t} = \frac{\overline{x_1} - \overline{x_2}}{\sqrt{\frac{s_{x1}^2 + s_{x2}^2}{n}}}, \dot{F} = \frac{s_{x1}^2}{s_{x2}^2}, \tag{4.3}$$

where $\overline{x_1}, \overline{x_2}$ are the sample means and s_{x1}, s_{x2} are the sample standard deviations.

The course of action was as follows:

Step 1: $m = 10^5$ pairs of samples both of size $n = 60$ were drawn from $EECK(4, 627, 1.96)$ (for negative excess kurtosis) and $EECK(3.669, 1.3)$ (for positive excess kurtosis) general populations.

Step 2: These pairs of samples were consecutively, converted into pairs of $\dot{t}_v$ statistics and $\dot{F}_v$ statistics, $v = 1, 2, ..., m$.

Step 3: Sets of values of $\dot{t}_v$ and $\dot{F}_v$ statistics were stored in two matrices named T and F.

Step 4: The matrices were sorted in ascending order and served to determine two empirical CDFs namely $\Theta_t\left(\dot{t_v}\right)$ and $\Theta_F\left(\dot{F_v}\right)$.

Step 5: Probability papers were employed to check whether the above empirical CDFs fit the Student and Fisher-Snedecor distributions.

Figures 8 and 9 show empirical CDFs of Step 4 plotted on the Student and Snedecor probability papers, when samples were drawn from $EECK(4, 627, 1.96)$ and $EECK(3.669, 1.3)$, appropriately. These probability papers were constructed in the same way as the Normal probability is constructed.

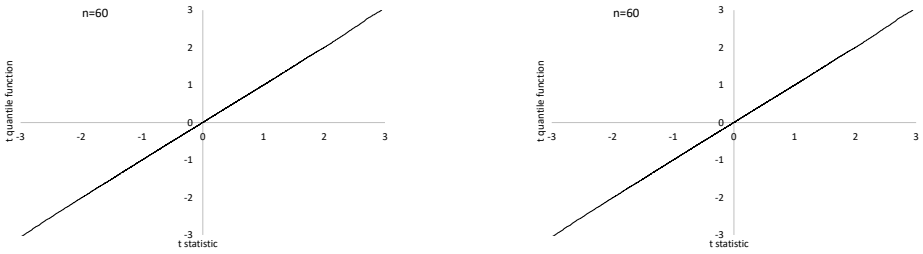

Figure 8: Empirical CDFs of Step 4 plotted on the Student and Snedecor probability paper. Case of negative excess kurtosis values

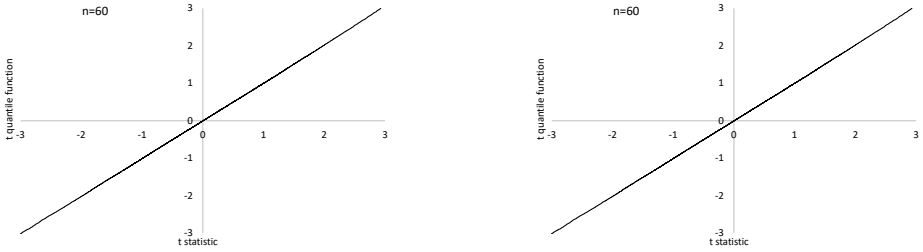

Figure 9: Empirical CDFs of Step 4 plotted on the Student and Snedecor probability paper. Case of positive excess kurtosis values

It turns out that the empirical distribution in question perfectly fit straight lines that relevant theoretical distributions. Thus, we can conclude that Student and Fisher-Snedecor tests may be applied even as population distributions are of negative (see Figure 8) or positive (see Figure 9) excess kurtosis.

4.2. Fitting distributions to data

Symmetric distributions have limited use in fitting the distributions to data (e.g. normal distribution). However, the situation looks much better when we use their mixture (e.g. compound normal distribution).

For the purposes of this subsection, we extend the domain of the $EECK(p,q)$ from $[-1,1]$ to $[-a,a](a \in R)$. PDF of the modified $EECK(p,q)$ distribution denoted as $EECK2(x,a,p,q)$ has the form
(4.4)

$$EECK2\,(x;a,p,q) = \frac{\int_{-a}^{a}\left[1-\left(\frac{|x|}{a}\right)^{q}\right]^{p}dx}{2\int_{0}^{a}\left[1-\left(\frac{|u|}{a}\right)^{q}\right]^{p}du}, x \in \begin{cases}(-a,a) & \text{if } -1<p<0\\ [-a,a] & \text{if } p\geq 0\end{cases}$$

In this subsection, we present real data examples to demonstrate a flexibility of the $EECK(p > -1, q > 0)$ distribution in the mixed variant. PDF of the compound EECK (CEECK) distribution is given by

$$\begin{aligned}(4.5)\quad CEECK\,(x;a,p_1,q_1,p_2,q_2,\omega) &= \omega EECK2\,(x;a,p_1,q_1)\\ &\quad + (1-\omega)\,EECK2\,(x;a,p_2,q_2)\end{aligned}$$

The estimation of the model parameters is carried out by the maximum likelihood method. To avoid local maxima of the logarithmic likelihood function, the optimization routine is run 100 times with several different starting values that are widely scattered in the parameter space. The KS GoFT was used for model fitting, while the AIC, BIC and HQIC were used for model comparisons. The p-values for the KS GoFT calculated as follows. First, we obtain the values of the KS test statistics (denoted ST) for true values of parameters $\widehat{\Theta}$ based on the sample $x_{(1)}, x_{(2)}, ..., x_{(n)}$. In the next step we simulate 10^3 samples $x'_{(1)}, x'_{(2)}, ..., x'_{(n)}$ from the given distribution with true values of parameters $\widehat{\Theta}$. For each sample, we calculate the values of the KS test statistics (denoted ST^s). Finally, the p-value is calculated as $p \approx \#\left\{i : ST_i^s > ST\right\} 10^{-3}$.

Real data examples

The first data set presents temperature dynamics of beaver Castor canadensis in north-central Wisconsin [25]. Body temperature was measured by telemetry every 10 minutes from one period of less than a day. The data consists of 114 observations of the variable "measured body temperature in degrees Celsius" and are available in the R software with code beaver1[3].

The second data set contains statistics, in arrests per 100,000 residents for assault in each of the 50 US states in 1973 [22]. The data consisting of 50 observations are available in the R software with code USArrests[2].

The models selected for comparison with the $CEECK\,(a,p_1,q_1,p_2,q_2,\omega)$ are:

- the compound ECK (CECK):
  $f_{CECK}(x; a, p_1, p_2, \omega) = \omega \frac{\left(1-\frac{x^2}{a^2}\right)^{p_1}}{aB(0.5,p_1+1)} + (1-\omega) \frac{\left(1-\frac{x^2}{a^2}\right)^{p_2}}{aB(0.5,p_2+1)}$
- the compound normal (CN):
  $f_{CN}(x; a_1, b_1, a_2, b_2, \omega) = \omega\phi(x; a_1, b_1) + (1-\omega)\phi(x; a_2, b_2)$
- the compound Laplace (CL):
  $f_{CL}(x; a_1, b_1, a_2, b_2, \omega) = \frac{\omega}{2b_1} \exp\left[\exp\left(-\frac{|x-a_1|}{b_1}\right)\right] + \frac{1-\omega}{2b_2} \exp\left[\exp\left(-\frac{|x-a_2|}{b_2}\right)\right]$,
- the compound Cauchy (CC):
  $f_{CC}(x; a_1, b_1, a_2, b_2, \omega) = \frac{\omega}{\pi b_1\left[1+\left(\frac{x-a_1}{b_1}\right)^2\right]} + \frac{1-\omega}{\pi b_2\left[1+\left(\frac{x-a_2}{b_2}\right)^2\right]}$
- the compound logistic (CLOG):
  $f_{CLOG}(x; a_1, b_1, a_2, b_2, \omega) = \frac{\omega \exp\left(\frac{x-a_1}{b_1}\right)}{b_1\left[1+\exp\left(\frac{x-a_1}{b_1}\right)^2\right]} + \frac{(1-\omega)\exp\left(\frac{x-a_2}{b_2}\right)}{b_2\left[1+\exp\left(\frac{x-a_2}{b_2}\right)^2\right]}$.

Tables 10 and 11 present values of the MLEs, log-likelihood function l, information criteria, KS test statistics and p-value for the first and second data set, respectively. The lowest values are in bold. The values of standard errors (calculated in the R software) for some parameters in the CEECK models are surprisingly large compared to other models. These values for the first data set are smaller than for the second data set. Figure 10 presents histograms, estimated PDFs of the analyzed models for the first (left) and second (right) data sets.

The CLOG model is the best in terms of the AIC, BIC and HQIC values and the CEECK model is distinguished in terms of the KS GoFT. It has the lowest KS test statistics and the highest p-value (see Table 10). The CEECK model is the best in terms of the AIC, BIC and HQIC values and the CL model is distinguished in terms of the KS GoFT. It has the lowest KS test statistics and the highest p-value (see Table 11). Based on the graphical and the numerical results, the CEECK distribution is considered as one of the best models for the analyzed data sets.

5. Conclusions

The article presents the extended easily changeable kurtosis (EECK) distribution, the special cases of which are the ECK, uniform and triangle distributions. The

Model	MLEs	AIC	BIC	HQIC	KS (p-value)
CEECK	$\hat{a} = 4.151(1.144), \hat{p}_1 = 2.039(1.981)$ $\hat{q}_1 = 0.700(0.827), \hat{p}_2 = 8958.252(33.333)$ $\hat{q}_2 = 5.371(0.623), \hat{\omega} = 0.660(0.177)$	321.570	337.987	328.233	**0.040 (0.978)**
CECK	$\hat{a} = 5.010(3.732), \hat{p}_1 = 5.413(11.662)$ $\hat{p}_2 = 55.361(95.471), \hat{\omega} = 0.484(0.162)$	318.331	329.275	322.773	0.041 (0.964)
CN	$\hat{a}_1 = -2.700(0.025), \hat{b}_1 = 0.042(0.017)$ $\hat{a}_2 = 0.071(0.086), \hat{b}_2 = 0.906(0.062)$ $\hat{\omega} = 0.026(0.015)$	319.489	333.170	325.041	0.084 (0.324)
CL	$\hat{a}_1 = -0.580(0.022), \hat{b}_1 = 0.722(0.326)$ $\hat{a}_2 = 0.144(0.010), \hat{b}_2 = 0.663(0.107)$ $\hat{\omega} = 0.201(0.127)$	320.786	334.467	326.338	0.087 (0.277)
CC	$\hat{a}_1 = -0.581(0.187), \hat{b}_1 = 0.353(0.133)$ $\hat{a}_2 = 0.226(0..095), \hat{b}_2 = 0.369(0.075)$ $\hat{\omega} = 0.294(0.149)$	336.771	350.452	342.324	0.103 (0.142)
CLOG	$\hat{a}_1 = 0.045(0.080), \hat{b}_1 = 0.492(0.040)$ $\hat{a}_2 = -2.700(0.029), \hat{b}_2 = 0.026(0.012)$ $\hat{\omega} = 0.975(0.015)$	**314.636**	**328.317**	**320.188**	0.050 (0.877)

Source: own material.

Table 10: Results of estimation for the first data set. The respective standard errors are in parentheses

Model	MLEs	AIC	BIC	HQIC	KS (p-value)
CEECK	$\hat{a} = 2.040(0.070), \hat{p}_1 = 183.915(34.654),$ $\hat{q}_1 = 378.415(68.096),$ $\hat{p}_2 = 389.387(86.483),$ $\hat{q}_2 = 23.107(9.233), \hat{\omega} = 0.203(0.141)$	**139.901**	**151.373**	**144.270**	0.088 (0.687)
CECK	$\hat{a} = 9.802(0.154), \hat{p}_1 = 32.874(0.613),$ $\hat{p}_2 = 63.054(8.567), \hat{\omega} = 0.356(0.078)$	149.929	157.577	152.841	0.136 (0.215)
CN	$\hat{a}_1 = -0.637(0.182), \hat{b}_1 = 0.567(0.125),$ $\hat{a}_2 = 1.089(0.241), \hat{b}_2 = 0.473(0.169),$ $\hat{\omega} = 0.631(0.122)$	142.002	151.562	145.643	0.072 (0.853)
CL	$\hat{a}_1 = 0.999(0.023), \hat{b}_1 = 0.415(0.126),$ $\hat{a}_2 = -0.693(0.022), \hat{b}_2 = 0.473(0.107),$ $\hat{\omega} = 0.392(0.089)$	143.930	153.490	147.570	**0.061 (0.944)**
CC	$\hat{a}_1 = -0.650(0.129), \hat{b}_1 = 0.404(0.114),$ $\hat{a}_2 = 1.025(0.080), \hat{b}_2 = 0.223(0.112),$ $\hat{\omega} = 0.655(0.101)$	156.244	165.805	159.885	0.081 (0.767)
CLOG	$\hat{a}_1 = -0.617(0.157), \hat{b}_1 = 0.355(0.074),$ $\hat{a}_2 = 1.099(0.163), \hat{b}_2 = 0.262(0.088),$ $\hat{\omega} = 0.648(0.103)$	143.369	152.929	147.009	0.072 (0.880)

Source: own material.

Table 11: Results of estimation for the second data set. The respective standard errors are in parentheses

new proposal tends to the normal distribution. The EECK, like the ECK, belongs to the family of symmetric, unimodal distributions, defined in the finite domain with excess kurtosis values on infinite interval. The obtained results demonstrate that the EECK distribution can be extremely useful when we want to seamlessly test GoFT's ability to detect deviations from normality by modeling of negative

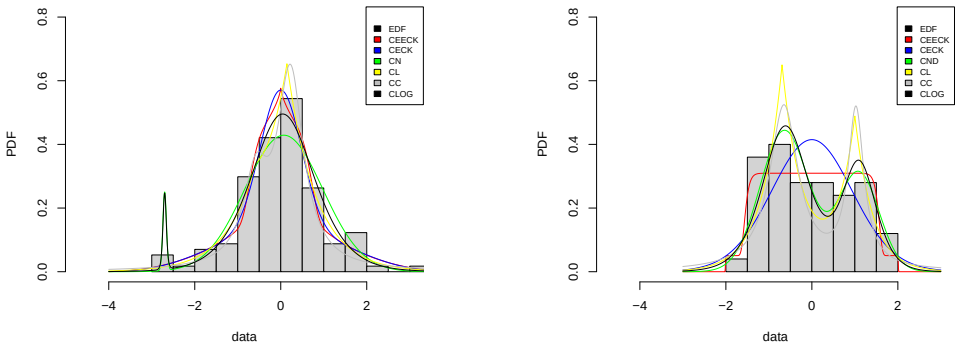

Figure 10: Histograms and estimated PDF of analyzed models for first (left) and second (right) data sets

or positive excess kurtosis. Student and Fisher-Snedecor tests may be applied even as population distributions are of negative or positive excess kurtosis. Real data example demonstrates that the $EECK(p, q)$ distribution in the mixed variant is flexible and competitive model that deserves to be added to the existing distributions in data modeling. The information presented in the article shows that the proposed distribution deserves to be added to the symmetric distribution family.

REFERENCES

[1] Ashour, S.K., Eltehiwy, M.A. (2013). Transmuted exponentiated modified Weibull distribution, *International Journal of Basic and Applied Sciences*, **2(3)**, 258—269.

[2] Azzalini, A. (1985). A class of distributions which includes the normal ones, *Scandinavian Journal of Statistics*, **2(12)**, 171—178.

[3] Balakrishnan, N. (1992). Handbook of the Logistic Distribution, *Marcel Dekker, New York*.

[4] Birnbaum, Z,W. and Saunders, S.C. (1969). A new family of life distributions, *Journal of Applied Probability*, **6(2)**, 319—327.

[5] Bolfarine, H.; Martínez-Florez, G. and Salinas, H.S. (2018). Bimodal symmetric-asymmetric power-normal families, *Communications in Statistics-Theory and Methods*, **47(2)**, 259–276.

[6] Buchanan, K., Wheeland, S. (2022). Comparison of the Quadratic U and Inverse Quadratic U Sum-Difference Beampatterns, *In 2022 IEEE International Symposium on Antennas and Propagation and USNC-URSI Radio Science Meeting*, 1828–1829).

[7] Bucher, J.L. (2012). The metrology handbook. Second Edition. *ASQ Quality Press*.

[8] Dekking, F.M., Kraaikamp, C., Lopuhaä, H.P., Meester, L.E. (2005). A Modern Introduction to Probability and Statistics: Understanding why and how (Vol. 488). London Springer.

[9] Edwards, A.W.F. (2000). Gilberts sine distribution. *Teaching Statistics*, **22(3)**, 70–71.

[10] Freimer, M., Kollia, G., Mudholkar, G.S., Lin, C.T. (1988). A study of the generalized Tukey lambda family. *Communications in Statistics-Theory and Methods*, **17(10)**, 3547–3567.

[11] Gibbons, J.F. and Mylroie, S. (1985). Estimation of impurity profiles in ion-implanted amorphous targets using joined half-Gaussian distributions, *Applied Physics Letters*, **11(22)**, 568–569.

[12] Glen, S. Degenerate Distribution: Simple Definition and Examples. *From StatisticsHowTo.com: Elementary Statistics for the rest of us! https://www.statisticshowto.com/degenerate-distribution/*

[13] Gradshteyn, I.S. and Ryzhik, I.M. (2014). Table of integrals, series, and products, *Academic press*.

[14] Hassan, M. Y., Hijazi, R. H. (2010). A bimodal exponential power distribution, *Pak. J. Statist*, **26(2)**, 379–396.

[15] Johnson, N. L., Kotz, S., Balakrishnan, N. (1995). Continuous univariate distributions, volume 2 (Vol. 289). John Wiley and Sons.

[16] Ki, H., Choi, B., Chang, K. H., Lee, M. (2005). Option pricing under extended normal distribution. *Journal of Futures Markets: Futures, Options, and Other Derivative Products*, **25(9)**, 845–871.

[17] Kotz, S., Balakrishnan, N., Johnson, N. L. (2004). Continuous multivariate distributions, Volume 1 (Vol. 1). John Wiley and Sons.

[18] Moors, J.J.A. (1988). A quantile alternative for kurtosis, *Journal of the Royal Statistical Society: Series D (The Statistician)*, **1(37)**,25–32.

[19] Lévy, P. (1940). Sur certains processus stochastiques homogènes, *Compositio mathematica*, **7**, 283–339.

[20] Malachov, A.N. (1978). A cumulant analysis of random non-Gaussian processes and their transformations (in Russian). *Soviet Radio*. Moscow.

[21] Mardia, K.V., Jupp, P.E., Mardia, K.V. (2000). Directional statistics (Vol. 2), *Chichester: Wiley.*

[22] McNeil, D. R. (1977). Interactive Data Analysis, *New York, Wiley.*

[23] Nadarajah, S. (2005). A generalized normal distribution. *Journal of Applied Statistics*, **32(7)**, 685–694.

[24] Raab, D., Green, E. (1961). A cosine approximation to the normal distribution. *Psychometrika*, **26(4), 447–450**.

[25] Reynolds, P.S. (1994). Time-series analysis of beaver body temperatures. Chapter 11 of Lange, N., Billard, L., Conquest, L., Ryan, L., Brillinger, D. and Greenhouse J. (Eds.), Case Studies in Biometry, *Proc. Berekeley Symposium, Statist. Probability, Wiley, New York.*

[26] Rinne, H. (2010). Location-Scale Distributions – Linear Estimation and Probability Plotting Using MATLAB, p. 116.

[27] Ryan, B.,K. (2014). Theory and applications of aperiodic (random) phased arrays. PhD Thesis.

[28] Sulewski, P. (2021). Two-piece power normal distribution, *Communications in Statistics - Theory and Methods*, **50(11)**, 2619–2639.

[29] Sulewski, P. (2020). Modified Lilliefors goodness-of-fit test for normality, *Communications in Statistics - Simulation and Computation*, **51(3)**, 1199–1219.

[30] Sulewski, P. (2022). Normal distribution with plasticizing component, *Communications in Statistics – Theory and Method*, **51(11)**, 3806–3835.

[31] Sulewski, P. (2022). Easily Changeable Kurtosis Distribution, *Austrian Journal of Statistics*, https://www.ajs.or.at/index.php/ajs/article/view/1434.

[32] Temme, N.M. (2010). Voigt function. *NIST Handbook of Mathematical functions*

[33] Torabi, H.; Montazeri, N.H. and Grane, A. (1961). A test of normality based on the empirical distribution function, *SORT*, **1(40)**, 1, 55–88.

[34] Umarov, S., Tsallis, c., Steinberg, S. (2008). On a q-Central Limit Theorem Consistent with Nonextensive Statistical Mechanics, *Milan J. Math. Birkhauser Verlag*, **76**, 307–328.

[35] Von Neumann, J. (1951). Various techniques used in connection with random digits, *National Bureau of Standards Applied Mathematics Series*, **12**, 36–38.